Check for updates

Enzyme immobilization inside the porous wood structure: a natural scaffold for continuous-flow biocatalysis†

Christian Goldhahn, [ab] Josef A. Taut,[a] Mark Schubert,[ab] Ingo Burgert [ab] and Munish Chanana ⋆[abc]

Enzymes are often immobilized on solid supports to enable their recovery from reaction solutions, facilitate their reuse and hence increase cost-effectiveness in their application. Immobilized enzymes may even be used for flow-through applications in continuous processes. However, the synthesis of traditional immobilization scaffolds and immobilization techniques lack sustainability as they are often based on fuel-based materials and tedious synthesis- and immobilization approaches. Here, we present the natural material wood as a green alternative for enzyme immobilization. Its natural structure provides a mechanically stable porous scaffold with a high inner surface area that allows for directional flow-through of liquids. Enzymes were immobilized by nanoparticle-mediated adsorption, a simple, versatile and completely water-based process. The resulting wood–enzyme hybrids were intensely investigated for the model enzyme laccase. Reaction kinetics, as well as catalytic activities at various pH-values, temperatures, and ionic strengths were determined. The wood–enzyme hybrids could quickly and completely be removed from the reaction solution. Hence, they allow for multifold reusability. We show a series of 25 consecutive reaction cycles with a remaining activity in the last cycle of 90% of the maximal activity. Moreover, the anisotropic porosity of wood enabled the application of the hybrid material as a biocatalytic flow-through reactor. Flow-rate dependent productivity of a single-enzyme reaction was determined. Moreover, we show a two-step reaction cascade in continuous flow by the immobilization of the enzymes glucose oxidase and horseradish peroxidase. Therefore, the natural material wood proved to be a promising material for application in continuous-flow biocatalysis.

Introduction

Catalysts are the basis for the modern chemical industry. Many synthetic processes cannot be executed without them.[1,2] Besides conventional catalysts, which are mostly based on metals, enzymes are widely used as a greener alternative. These bio-catalysts are highly active and specific under mild reaction conditions and offer a huge variety of possible reactions.[3] Moreover, they are produced from natural resources, making them more sustainable than metal-based catalysts. Their application fields range from food, textile, and detergent industry to complex functional devices like bio-sensors.[4]

Enzymes work naturally as homogeneous catalysts in aqueous solutions. The resulting batch-processes bear certain

disadvantages. The removal of the enzymes can be tedious as they are dissolved in the reaction solution. Hence, enzymes are often only applied for single-use and stay behind as impurities in the reaction product. Furthermore, batch processes are *per se* less productive than continuous production methods.[5,6]

Immobilization of enzymes on solid supports is widely used to overcome these problems.[7] The immobilization enables simpler separation of the biocatalyst from the reaction solution as it converts the homogeneous nature of the dissolved enzyme molecules to a heterogeneous system.[8] Consequently, the resulting nano- or micro-hybrids can be separated from the reaction solution by established techniques like filtration or centrifugation. Furthermore, enzyme immobilization can be used to realize continuous-flow biocatalysis, combining the advantages of biocatalysis and continuous production.[9] In these approaches, enzymes are often coupled to powders or porous beats and subsequently randomly packed into a fixed bed reactor.[10–12] However, such reactors have uncontrolled fluid dynamics, resulting in inhomogeneous distribution of reactants and products, a broad residence time distribution, and low selectivity.[13] In addition, fixed bed reactors can exhibit

[a] *ETH Zürich, Institute for Building Materials, Stefano-Franscini-Platz 3, 8093 Zürich, Switzerland. E-mail: chananam@ethz.ch*

[b] *Empa – Swiss Federal Laboratories for Material Science and Technology, Cellulose & Wood Materials, Überlandstrasse 129, 8600 Dübendorf, Switzerland*

[c] *Swiss Wood Solutions AG, Stefano-Franscini-Platz 3, 8093 Zürich, Switzerland*

† Electronic supplementary information (ESI) available. See DOI: 10.1039/c9ra10633b

a high pressure drop. Hence, the structuration of the bed geometry is highly desirable to overcome these drawbacks.

The use of porous monoliths is one way to tackle these problems.[14,15] In this context, the term monolith depicts a continuous unitary structure that offers structured pores, high inner surface area, and low pressure drop for flow-through applications.[16,17] In addition to being used for conventional catalysis, they have been investigated as scaffolds for enzyme immobilization.[18–22] With such systems, effective continuous-flow biocatalysis is possible, for example for the production of biodiesel or fine chemicals.[23,24]

Generally, the materials used for these applications are either inorganic silica-based monoliths synthesized by sol–gel chemistry,[25,26] porous polymer networks,[27,28] or polymer–inorganic composites.[29] Hence, they require tedious synthetic processes as well as energy- and resource-intensive production methods, which calls for more sustainable alternatives.

In analogy to conventional monoliths, we propose the renewable resource wood as a suitable porous scaffold for enzyme immobilization and application in continuous-flow biocatalysis. Wood is a highly abundant and CO_2-storing resource that offers the necessary structural features for this purpose. At the micro level, wood's natural anatomy exhibits a bundle of unidirectional pores, which are aligned along the tree's axial direction and enable directional flow of liquids. Furthermore, wood is mechanically stable, easy to handle and to process, and offers a relatively high inner surface area.[30] Wood and wood-based functional materials have therefore recently been used for various flow-through applications. They comprise membranes for water filtration,[31–35] oil/water-separation,[36–38] and membranes with tunable flux.[63] Moreover, flow-through catalysis has been performed with a wood-based material. For this purpose, the wood was decorated with palladium nanoparticles to achieve catalytic dye degradation in the permeate.[39] Enzyme immobilization on wood, however, has never been reported.

Individual wood constituents have been used as scaffold materials for enzyme immobilization. For example the polyphenolic lignin, which is a side product of the paper industry, was used for the production of hydrogels on which enzymes were immobilized.[40,41] Another material that is derived from wood and has been used as scaffold for enzyme immobilization are cellulose nanofibers and nanocrystals.[42,43] However, these wood-derived materials are molecular or nano-sized components and have no intrinsic structure on the micro-level. Hence, they are not suited for continuous-flow biocatalysis without further processing.

We show the proof of concept for the application of wood as a scaffold material in continuous-flow biocatalysis. Enzyme immobilization on wood was achieved by gold nanoparticle mediated adsorption, an approach that we developed and applied on cellulose fibers in previous studies.[44,45] It is based on a two-step impregnation of wood with aqueous reaction solutions. The approach is easy, versatile, and requires no pre-modification of the enzyme or arduous cleaning or purification steps. This is in contrast to common production methods of heterogeneous biocatalysts by covalent grafting of the enzymes, for which such additional steps are essential. The resulting wood–gold–enzyme hybrids are easy to handle, offer a high reusability, and can be applied as flow-through reactors. Moreover, multi-step cascade reactions can be realized by immobilization of multiple enzymes. Hence, the material is a promising step towards greener heterogeneous biocatalysts.

Results and discussion

The immobilization of enzymes on wood was executed in a two-step process (Fig. 1). In a first step, poplar wood was prepared as a scaffold for enzyme immobilization by *in situ* gold reduction. Cylindrical samples of poplar wood with diameters of 16 mm were vacuum impregnated with chloroauric acid. Poplar is a hardwood species with a low density and high porosity as a result of a high amount of vessels (Fig. S1† shows the microstructure of poplar wood).[30] These vessels are pores with diameters of about 40 μm to 100 μm that are elongated in the
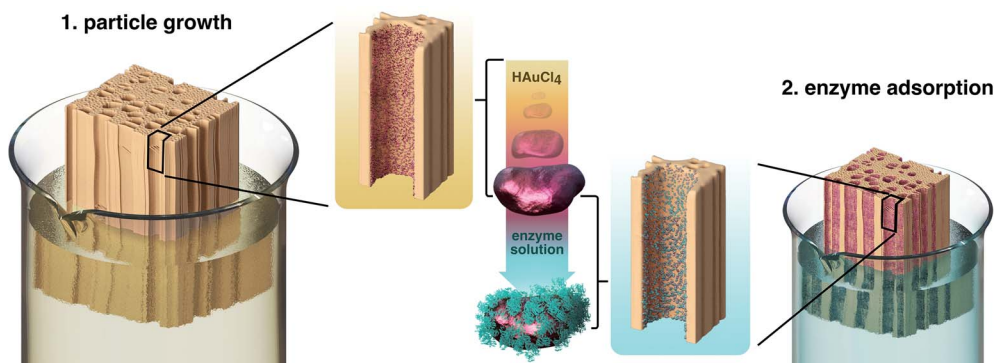

Fig. 1 Schematic illustration of the immobilization process of enzymes in hardwood. During the two-step process, the wood is first impregnated with chloroauric acid to induce the growth of gold nanoparticles inside the wood structure. In the course of the reaction, Au^{3+}-ions are reduced *in situ* by the wood cell walls and form a layer of particles on their surface. In a second step, the gold particle-impregnated wood is incubated with an enzyme solution. The enzymes robustly adsorb to the gold particles, leading to biocatalytic wood–gold–enzyme hybrids (wood@-Au@enzyme). The graphical overview does not specifically illustrate poplar wood.

axial direction of the tree. They can reach a length of several centimeters in poplar wood and are mainly responsible for the water-flow through the wood structure.[46,47] Hence, the sapwood of hardwoods can be impregnated more easily with reaction solutions compared to softwoods that do not have vessels. Moreover, the high amount of vessels leads to an easy flow-through with low pressure drop, which is beneficial for flow-through applications.[34,63]

Over the course of the reaction, the solution penetrates the porous wood structure, in which Au^{3+}-ions are then reduced to gold particles at the surface of wood cell walls. It was shown, that the cell wall component lignin can act as a reducing agent for noble metal ions.[39] As a result, wood–gold hybrids (wood@Au) are obtained that exhibit a violet color due to the characteristic plasmon resonance of the immobilized gold particles (Fig. 2A). We used gold for this purpose, as it offers two important advantages. Firstly, the gold ions can easily be reduced due to their high redox potential, so that lignin can function as a reducing agent and no additional reducing agent is necessary. Secondly, gold has a high affinity for protein

adsorption, which is important for the second immobilization step. Notably, the use of other potentially cheaper metals is conceivable, as many metals provide good protein adsorption. Depending on the metal's redox potential, an additional reducing agent might be necessary.

When the gold particle-impregnated wood samples were cut open, the violet coloring of the wood indicated that particles formed throughout the whole sample (Fig. 2A). However, the coloring gets less intense towards the inner part of the sample, showing that the particles are not uniformly distributed throughout the sample thickness. This is because the impregnation solution penetrates the samples mainly along the pore direction and gold ions are already reduced at the periphery and their concentration decreases towards the center. A sample thickness of 3 mm was determined to allow for a decent penetration with reaction solution through the whole sample.

The modified cell wall surface was investigated by scanning electron microscopy (SEM) of wood@Au samples. The micrographs show gold particles on the surface of the cell walls as bright spots due to their higher electron density. Overview
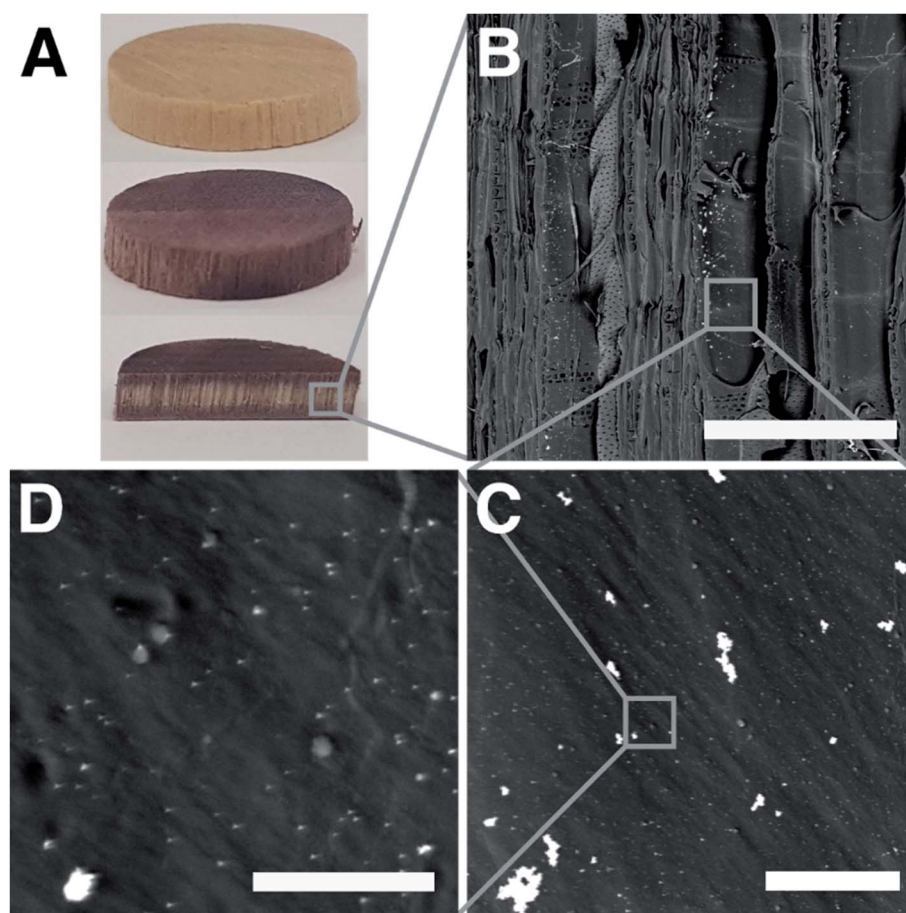

Fig. 2 (A) Photographs of native poplar wood (top), gold-impregnated poplar wood (center), and cut-open impregnated poplar wood (bottom). The gold particles that were induced during the first modification step cause a color change to violet. In the cut-open sample, the heterogeneity of the modification gets visible, which is caused by decreasing Au^{3+}-concentration towards the center of the sample. All samples have a diameter of 16 mm and a height of 3 mm. (B–D) SEM micrographs of poplar wood with increasing magnifications. The particles are well visible as bright spots on the inner surface of the wood cell walls. Particle clusters with sizes of several micrometers are visible, as well as individual particles with diameters below 100 nm. Scale bars depict 300 μm in (B), 10 μm in (C), and 3 μm in (D).

images show that the particles are mainly located on the inner cell walls of the vessels and that the overall microstructure and micro-porosity of the wood samples is not altered by the modification process (Fig. 2B). The sizes of the particles were determined by digital image analysis with the software ImageJ (Fig. S2†). A bimodality in the particle size is visible. On the one hand, individual small particles were detected with sizes below 100 nm (74.49 nm ± 26.21 nm). On the other hand, big particle agglomerates with sizes of several hundred nanometers and up to 5 micrometers are visible. In general, the *in situ* synthesis leads to heterogeneous particle sizes with a wide distribution. This is mainly caused by the heterogeneous surface morphology and chemistry of the wood cell walls. Another factor might be concentration gradients of the incubation solution while penetrating the wood structure.

In a second step, the enzymes were immobilized on the inner surface of poplar wood by adsorption. We chose the oxidoreductase laccase (lac) for the characterization of the system, as it offers a broad range of possible model reactions and proved to be suitable for immobilization by adsorption.[48]

The immobilization was achieved by vacuum impregnation of wood@Au samples with a solution of laccase in buffer (10 mM,

pH = 3). After impregnation, the final wood–gold–enzyme hybrids (wood@Au@lac) were washed three times with buffer solution and subsequently stored in buffer until they were used.

The amount of immobilized enzyme was determined by fluorescence spectroscopy. For this, the laccase was labeled with the fluorescent dye tetramethylrhodamine-5-6-isothiocyanate (TRITC) prior to the immobilization process. The fluorescence intensity of the impregnation solution was then measured before and after the impregnation and the amount of immobilized enzymes was calculated as the difference between these values. We found that $(0.17 \pm 0.37 \times 10^{-2})$ mg of enzyme were immobilized per wood sample. This equals 0.56 mg of enzyme per one gram of wood and 34.0% of the laccase provided in the impregnation solution. The adsorption efficiency is consistent with both our previous work on the immobilization of laccase on cellulose fibers and other studies investigating the immobilization of laccase by adsorption.[44,49,50] The amount of immobilized enzymes (0.56 mg g^{-1}) is lower than reported in literature. This is most likely due to the lower specific surface area of wood, compared to nano-sized or nanoporous materials, resulting in a lower accessible surface area per gram sample.
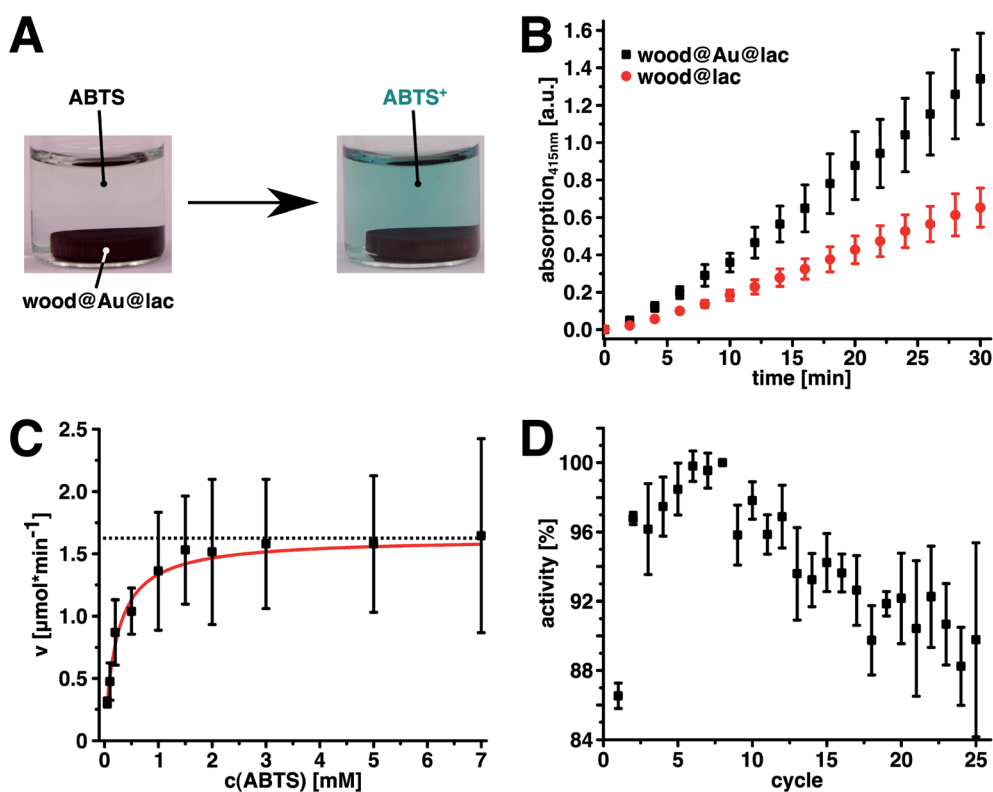

Fig. 3 (A) Photographs of wood@Au@lac in an ABTS solution in buffer (pH = 3) immediately after insertion of the sample (left) and after 30 minutes of reaction time (right). The immobilized laccase catalyzes the oxidation of ABTS to its greenish blue radical cation, proving successful enzyme immobilization. (B) Plot of the absorption of the reaction solutions at $\lambda = 415$ nm over time for laccase on impregnated wood (wood@Au@lac) and on native wood (wood@lac). Continuous product formation leads to a linear increase of absorption. The wood@Au@lac is about twice as active as the wood@lac. (C) Plot of the initial reaction velocities of the oxidation of ABTS by wood@Au@lac against the substrate concentration. The red line represents the hyperbolic fit of the data, which allows for the determination of the kinetic parameters K_M and v_{max} of the reaction. The dotted line represents v_{max}. (D) Plot of the relative activities of wood@Au@lac over 25 reaction cycles. The values are normalized to the maximal activity in the eighth cycle. The activity increases after the first cycle until it reaches a maximum in the eighth cycle, before it starts to decrease over the rest of the cycles. The remaining activity after the 25th cycle is 90% compared to the eighth cycle.

A successful immobilization of the enzyme was proven by catalytic activity measurements of the hybrids. We chose the oxidation of 2,2′-azino-bis(3-ethylbenzothiazoline-6-sulphonic acid) (ABTS) to its stable radical cation as a model reaction. This reaction can be enzymatically catalyzed by laccase and leads to a color change of the solution from colorless to a greenish blue (Fig. 3A). The increasing amount of reaction product can easily be detected and quantified photometrically by measuring the light absorption of the reaction product at the local absorption maximum (Fig. S3,† $\lambda = 415$ nm, $\varepsilon_{415}(ABTS^+) = 3.60 \times 10^4$ L mol^{-1} cm^{-1}).[51] Fig. 3B shows the linear increase of reaction product that indicates the catalytic activity of wood@Au@lac and, hence, successful enzyme immobilization. We evaluated enzyme leaching by testing the catalytic activity of the washing solution of the last washing cycle. No catalytic activity (ABTS-oxidation) could be detected in this solution. Hence, we conclude that the enzymes are robustly bound and no significant enzyme desorption takes place after washing. In a control experiment, native wood without gold particles was impregnated with laccase in the same way as the wood–gold–hybrids. These samples also show catalytic activity (Fig. 3B, red dots), indicating that enzymes were adsorbed to the native wood structure as well. However, the samples without gold particles showed leaching of enzyme and a poor reusability, since no robust binding of the enzyme took place. Hence, the resulting activity is only half as high as for wood@Au@lac. Therefore, we conclude that the gold particle-loaded inner wood surface, in comparison to the bare inner wood surface, provides a higher affinity for enzymes. Hence, it allows for easy and robust enzyme immobilization inside the wood structure, which is not possible to this extent in native wood. This result is in agreement with our prior work, in which we showed the immobilization of enzymes and other proteins on colloidal metal surfaces.[44,45,52–55] These proteins bind robustly to the surfaces, without any detectable leaching. If enzymes are attached, they remain their catalytic activity after the adsorption.[45]

We determined the kinetic parameters of the ABTS-oxidation catalyzed by wood@Au@lac to gain further insight into the catalytic activity of the system and to compare them with the native enzyme. The characteristic Michaelis constant K_M as well as the maximal reaction velocity v_{max} were obtained by plotting the reaction rates at different substrate concentrations, followed by a hyperbolic fit of the data (Fig. 3B and Table 1). The Michaelis constant is the substrate concentration at which $0.5v_{max}$ is reached. It relates to the binding affinity of the substrate to the enzyme, where lower values of K_M represent a higher affinity. Moreover, K_M is independent of the enzyme

concentration. Hence, K_M-values of various enzyme systems (immobilized, native) can directly be compared to each other. The wood@Au@lac samples showed a K_M-value of 0.219 ± 0.014 mM. This value is about twice as high as for laccase immobilized by nanoparticle-mediated adsorption on cellulose fibers and about six times as high as the K_M-value of free laccase.[44] It is known that enzyme immobilization can lead to increased apparent K_M-values, mainly due to structural changes of the enzyme during immobilization,[56] as well as the build-up of an unstirred solvent layer around the immobilization surface. This so called Nernst layer is product rich and substrate depleted and hence leads to slower reaction kinetics.[57,58] Another factor that decreases the reaction speed for wood@Au@lac might be diffusion limitations due to the porous structure of poplar wood.[59] This means that a substrate has to diffuse inside the wood pores to reach the enzymes immobilized on the inner surface of the structure. Furthermore, product formed inside the wood pores has to diffuse out of the structure after the reaction to be detectable by photospectrometry. The time needed for this diffusion process could be another limiting factor for the reaction kinetics. Moreover, the pore-size of the wood could decrease due to swelling of the wood structure during the process.[34] This would further increase diffusion limitations. However, such a behavior is very unlikely in the case of this measurements, as they were executed with samples that were already kept in a water-saturated state for more than 24 hours. Hence, the swelling is already finished, at the start of the activity measurement.

Moreover, we determined the turnover number k_{cat} of the system. This parameter can be calculated from v_{max} ($v_{max} = (1.626 \pm 0.061)$ µmol min^{-1}) by normalizing it over the enzyme concentration. It gives the amount of substrate that is formed by one enzyme over a certain duration. It can also be compared directly to the turnover numbers of other enzyme systems. The turnover number of wood@Au@lac is 15.21 s^{-1}. This is approximately 25% lower than for laccase immobilized on cellulose fibers. Again, the diffusion limitations could be a reason for the lower value, as a cellulose fiber surface is better accessible than the inner surface of the bulk wood structure. The turnover number of free laccase is twelve times higher than the one of wood@Au@lac. In general, it is known that immobilized enzymes exhibit slower kinetics as their free counter parts. The reason for this are manifold and can be attributed to diffusion limitations, blocking of the active site of a part of the immobilized enzymes due to non-optimal orientation of the macromolecules during immobilization, or changes in the 3D-structure of the enzyme caused by the attraction forces between enzyme and scaffold. Approaches to increase the performance of immobilized enzyme can be stabilizing modifications of the biocatalysts prior to the immobilization or more site-specific binding to avoid blocking of the active center. As these techniques come with additional synthesis steps, we decided against such measures to keep the process as simple as possible.

Although wood@Au@lac shows slower kinetics than free laccase and laccase on cellulose fibers, it offers distinct advantages over these systems. First of all, the system provides a very

Table 1 Kinetic parameters of immobilized and free laccase ($M_{lac} = 97$ kDA).[60]

	K_M [mM]	v_{max} [µmol min^{-1}]	k_{cat} [s^{-1}]
Wood@Au@lac	0.219	1.63	15.21
Lac on cellulose fibers[44]	0.105	2.27	19.22
Free laccase[44]	0.037	0.57	200.33

high reusability. In a batch process, the samples were immersed in a reaction solution of ABTS. After the reaction took place for ten minutes, the samples could readily be removed from the solution. The mechanical stability of the wood samples ensures that there is no loss of catalyst during handling or removal. Furthermore, no residual gold particles could be detected in the reaction solutions. After rinsing the samples, they could be reused for the next reaction cycle. The solid and mechanically stable wood structure offers the possibility to easily process the sample and completely remove the enzymes from the reaction solution. Hence, more tedious separation techniques such as filtration or centrifugation are omitted. In contrast, free enzymes are hard to remove from the product solution due to their homogeneous nature and can remain as an impurity in the final product. Laccase on cellulose fibers also provides easy removability from the reaction solution. However, the fibers only hold together by physical entanglement and do not offer a mechanically stable support. This can lead to remaining fibers or fiber parts in the product solution and results in a loss of enzyme.[44]

We executed 25 consecutive reaction cycles and measured the amount of product after each cycle, which directly correlates to the enzymatic activity. The activity was then normalized to the maximal activity in the eighth cycle, which equals 100%. Fig. 3C shows the result of the experiment. Interestingly, the activity increased after the first cycle until it reached its maximum in cycle eight. From there on, the activity continuously decreased to a value of approximately 90% in the 25th reaction cycle. The increase in activity in the first eight cycles is potentially caused by the already mentioned diffusion effects. In the beginning of the first cycle, the concentration of substrate (ABTS) is low inside the wood structure. Hence, a certain duration is needed for the diffusion of ABTS into the wood structure to establish the equilibrium concentration and reaction rate. Furthermore, the product formed inside the wood structure, has to diffuse to the outside to become detectable. Probably, the time needed until an equilibrium state is reached comprises the first eight reaction cycles. Subsequently, a decreased activity over time represents the typical behavior for immobilized enzymes. The amount of 25 cycles that can be realized is, however, quite remarkable. In the 25th cycle, wood@Au@lac is still more active than in the first cycle and has about 90% remaining activity referred to the maximum in the 8th cycle. Laccase on cellulose fibers, in comparison, only
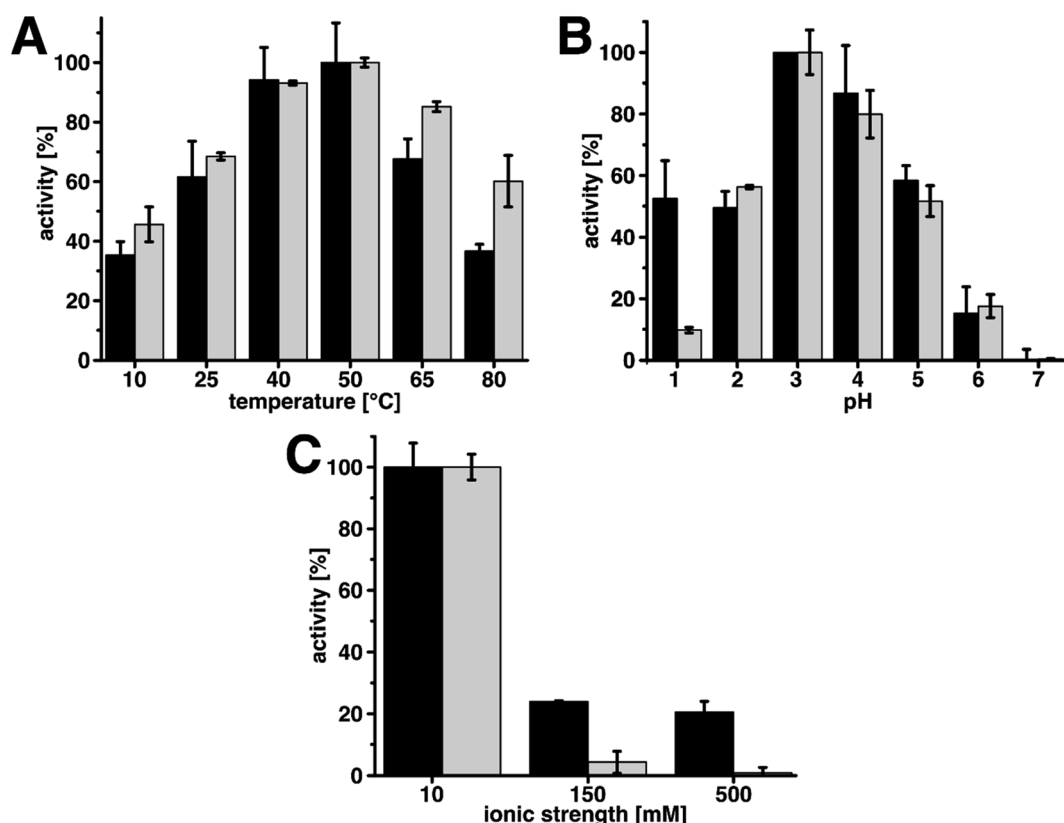

Fig. 4 Plots of relative activities of wood@Au@lac (black) and free laccase (grey) under various environmental conditions. In each plot the values were normalized to the highest values, which represent 100% relative activity. (A) Relative activities at multiple temperatures. Immobilized and free laccase show similar activities with a maximum at 50 °C in both cases. Free laccase shows higher relative activities at temperatures below and above the optimum. (B) Relative activities at multiple pH-values. Both systems show similar activities with a maximum at pH 3. The only notable difference is at pH 1, at which wood@Au@lac performs significantly better than free laccase. (C) Relative activities at three different ionic strengths. The activity decreases with increasing ionic strength in both cases. Immobilized laccase shows higher activities than free laccase for increased ionic strength.

achieves a remaining activity of 24% after 20 reaction cycles, which is also the potential achieved by similar systems of immobilized laccase.[44,61] In this regard, the mechanically stable monolithic wood structure shows advantages over loosely entangled fibers. The easy removability, mechanical robustness and the multifold reusability of the catalyst can be relevant advantages for industrial bulk processes as they increase the cost-effectiveness of the enzyme application.

Moreover, for practical applications it is of interest, how the catalyst performs under various environmental conditions such as varying temperature, pH, or ionic strength. We investigated the performance of wood@Au@lac under these influences and compared the relative activities to the ones of free laccase (Fig. 4). For all the measurements, the maximal activity was set as 100% and the other values were normalized to these values.

In case of varying temperatures, wood@Au@lac exhibited the activity maximum at 50 °C. This is the same value as for free laccase and in agreement with literature.[60] For temperatures below and above the maximum, the activity decreased for wood@Au@lac as it did for free laccase. While for lower temperatures the activities of free and immobilized laccase were in the same ranges, for higher temperatures (65 °C and 80 °C), the activity of wood@Au@lac was significantly lower than the one of free laccase. Hence, wood@Au@lac can be considered less suitable in particular for higher application temperatures.

Measurements of pH-dependent activities showed that the optimum was at pH 3 for both free and immobilized laccase. The activities decreased for pH-values below and above 3 and no activity remained at pH 7. The maximum, as well as the decreasing activities for higher and lower pH-values are in accordance with literature.[60] Only at pH 1, wood@Au@lac showed a divergent behavior from free laccase. At this value, the immobilized laccase had a remaining activity of approximately 53% of the maximal activity. This is significantly higher than the 10% activity which remained for free laccase at this value. The effect is potentially caused by a buffering influence of the wood structure at this low pH. Wood cell wall components carry a high amount of OH-groups, which can be protonated at low pH-values. This could lead to a lower H^+-ion concentration and hence higher apparent pH inside the wood structure.

Moreover, we investigated the activity of the catalyst at various ionic strengths. We chose ionic strength values of 10 mM, 150 mM, and 500 mM. The lowest value of 10 mM is the ionic strength caused by the buffer in the reaction solution. An ionic strength of 150 mM is similar to physiological conditions and 500 mM represents a rather high ionic strength as it might occur in industrial processes. In general, additional ions in the reaction solution can destabilize the enzyme structure resulting in a loss of activity. In both cases, the ionic strength was established by the addition of sodium chloride (NaCl). The results show that both systems have their maximal activity at the lowest ionic strength. For higher ionic strengths, the activity of free laccase rapidly decreased. At 150 mM only 4% of the maximal activity remained and at 500 mM almost no activity was left (1%). The immobilized laccase, on the contrary, appears to be more robust than the free enzyme. At an ionic strength of 150 mM an activity of 24% and at 500 mM an activity of 21%

remained. The resilience of wood@Au@lac against ionic strength may be caused by stabilization of the enzyme structure during immobilization or again a buffering effect of the wood structure. It is conceivable that ions adsorb to the wood surface, leading to a lower apparent ionic strength in the solution. The resistance against high ionic strengths can be beneficial for industrial applications, as in industrial processes a rather high ionic strength of the reaction solution is not unusual.

In terms of applications, continuous processes are favored against discontinuous bulk reactions. In this regard, the wood structure is particularly suited as it enables a directional flow due to its anisotropic pores. Hence, it is possible to use wood@Au@lac as a flow-through reactor (Fig. 5A). The substrate solution can readily penetrate the structure along the pore direction. The flow-through is thereby mainly managed by the larger pores of the vessels. Inside the structure, the substrate comes into contact with the immobilized enzymes on the wood cell walls, where it is biocatalytically transformed into the product. As the wood offers a mechanically stable porous structure, it can act as a flow-through reactor by itself. Hence, the samples can be put directly into the flow of the reaction solution and no further implementation, for example into a fixed-bed reactor, is necessary. The product rich permeate can then be collected on the downstream side of the sample.

We executed this process with a customized flow-through set-up, which mainly consists of a peristaltic pump, which can establish a continuous flow, and a customized sample holder that can tightly hold multiple samples at once and ensures a flow of the substrate solution through the samples (Fig. S4†).

Flow-through experiments were executed with wood@-Au@lac at three different flow-rates (4, 6, and 8 mL min^{-1}). For every trial, three samples were used at once to increase the amount of enzyme and the contact times between substrate solution and biocatalyst (Fig. S4B†). We determined the amount of product during the first ten minutes by UV/Vis spectroscopy. The results are shown in Fig. 5B. The graph shows a linear increase of product for all flow-rates. This confirms that continuous-flow biocatalysis can successfully be executed with wood@Au@lac. Furthermore, the data show no increase of the reaction velocity over time, as it was observed in the former reaction cycles measurements. This indicates that the transport of substrate inside the wood structure and of product out of the wood structure is governed by the capillary flow and not by diffusion. Hence, equilibrium conditions are established quicker than under diffusion controlled conditions.

A linear fit of the plot gives the production rate in μmol min^{-1}. Table 2 provides an overview over the production rates and the product concentrations in the permeate for each flow-rate. The product concentration in the permeate decreases with increasing flow-rate. This is caused by shorter contact times between the substrate solution and the catalyst for increasing flow-rates. However, this effect is compensated by the higher output at increasing flow-rates. This means that the higher the flow-rate, the higher the amount of permeate. For example, 8 mL min^{-1} of permeate with a low product concentration yield a similar overall amount of product as 4 mL min^{-1} of permeate with a higher product concentration. Nevertheless,
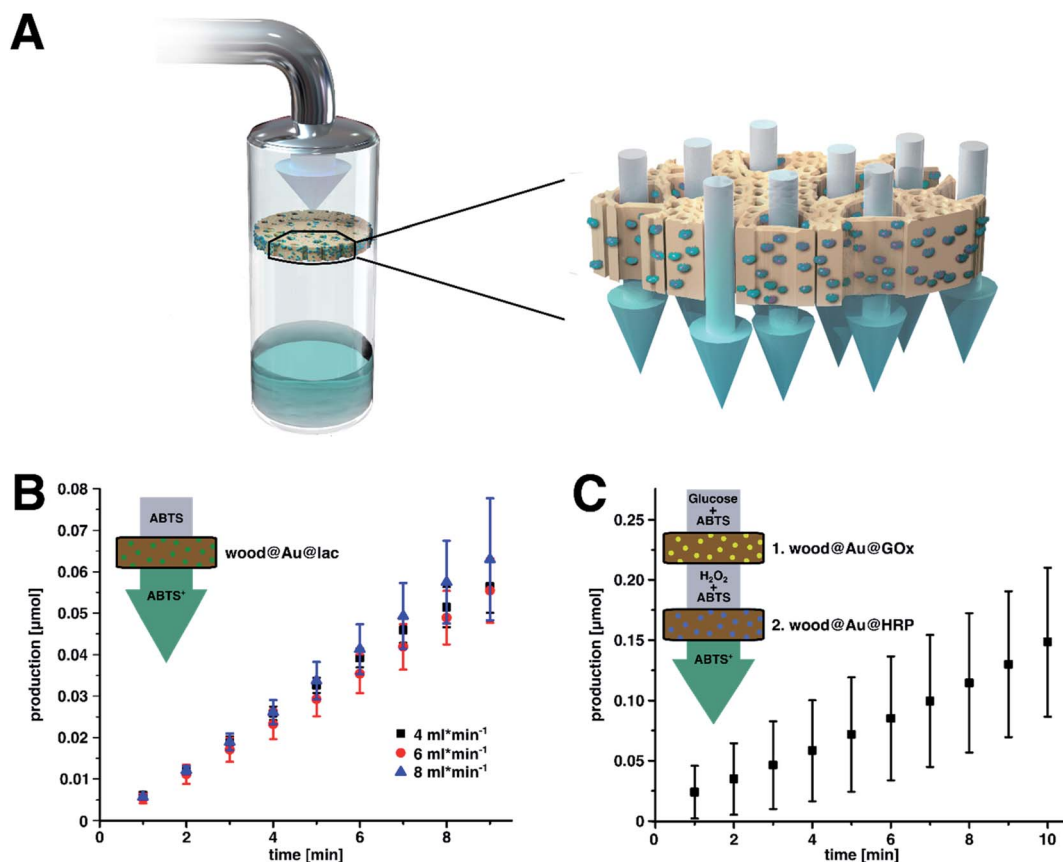
Fig. 5 (A) Schematic illustration of the flow-through reaction. The reaction solution flows through the wood due to its natural anisotropic porous structure. Inside the wood, the solution comes in contact with immobilized enzyme and hence the biocatalytic reaction takes place. (B) Plot of the production of oxidized ABTS over time by the flow-through of wood@Au@lac for various flow-rates. There are no big differences in the amount of product. This means that for higher flow-through rates, the lower product concentration caused by shorter contact times are compensated by a higher permeate volume. (C) Plot of the production of oxidized ABTS over time by the flow-through of first wood@Au@Gox followed by wood@Au@HRP with a flow-rate of 4 mL min^{-1}. In this case, a two-step cascade reaction takes place, during which first hydrogen peroxide is formed from glucose by immobilized Gox. This reaction product of the first reaction then reacts with ABTS in a second step catalyzed by immobilized HRP.

Table 2 Production rates and product concentrations in the permeate for flow-through experiments with wood@Au@lac

Flow-rate [mL min^{-1}]	Production rate [10^{-3} μmol min^{-1}]	Product concentration [μmol L^{-1}]
4	6.42	1.61
6	5.88	0.98
8	6.03	0.75

a higher product concentration means higher yield and lower remaining amount of substrate and should hence be favored.

Furthermore, not only single-step reactions are possible by this procedure, but also multi-step reaction cascades. As the immobilization process is rather simple and thus versatile, it can also be applied for the immobilization of other enzymes. As a proof of concept, we immobilized the enzymes peroxidase from horseradish (HRP) and glucose oxidase from *Aspergillus niger* (Gox) with the same protocol as for laccase, resulting in the wood–gold–enzyme hybrids wood@Au@HRP and wood@Au@Gox, respectively. These enzymes can carry out a reaction cascade in the way that Gox first oxidizes glucose to glucono lactone under the production of hydrogen peroxide. In a second step, the hydrogen peroxide can be used by HRP as a co-substrate for the oxidation of a suitable substrate, as for example ABTS.

We executed the flow-through cascade reaction by mounting three samples of wood@Au@Gox, followed by three samples of wood@Au@HRP (Fig. S4B†), so that the substrate solution (glucose and ABTS in buffer, pH = 7) comes into contact with immobilized Gox first and is thereafter transported to the immobilized HRP. In this way, hydrogen peroxide is produced in the first three samples (wood@Au@Gox) and is then consumed by the second three samples (wood@Au@HRP) to oxidize ABTS. The amount of product (ABTS$^+$) in the permeate can be determined by UV/Vis absorption. It is noteworthy that hydrogen peroxide could degrade lignin and hemicelluloses in the wood structure. We did not investigate this effect, but we assume that due to low hydrogen peroxide concentration and short contact times no critical disintegration takes place.

Table 3 The buffers that were used for the pH-dependent activity measurements

pH	Buffer
1	KCl/HCl
2	KCl/HCl
3	$Na(CH_3COO)/CH_3COOH$
4	$Na(CH_3COO)/CH_3COOH$
5	$Na(CH_3COO)/CH_3COOH$
6	$KH_2PO_4/NaOH$
7	$KH_2PO_4/NaOH$

The results of the measurement are plotted in Fig. 5C. The linear increase of product over time indicates a successful continuous-flow reaction cascade. Again, a linear increase of product indicates that the reaction equilibrium is quickly established due to flow-through conditions. The production rate is 14.77×10^{-3} µmol min^{-1}. However, the absolute values of the production rates cannot be compared between the cascade system and the single reaction system with laccase. Nevertheless, the proof that the approach can be transferred to other enzymes and that it is possible to catalyze multi-step cascade reactions in continuous flow is a promising result when it comes to potential applications of the method, as multi-step continuous-flow synthesis is highly attractive for the production of drugs or commodity chemicals.[62] Enzymes immobilized on wood offer an easy, versatile, and convenient system for the realization of such multi-step synthetic pathways. Samples with different immobilized enzymes can thereby individually be combined and inserted into the reaction flow.

Conclusion and outlook

In this work, we presented the straightforward and versatile immobilization of enzymes on wood by nanoparticle-mediated adsorption. The enzyme laccase was successfully immobilized on wood, which was previously functionalized by *in situ* growth of gold particles inside the wood structure. The resulting wood–gold–enzyme hybrids were intensely investigated with regard to their reaction kinetics, catalytic activity under various environmental influences (temperature, pH, and ionic strength), reusability, and applicability as a flow-through heterogeneous biocatalyst.

The immobilized laccase proved to be catalytically active. The reaction kinetics were slower than for the free enzymes. Apart from that, the immobilized enzyme showed similar relative activities as the free enzyme under most pH conditions and temperatures at and below 50 °C. The immobilized enzyme, though, proved to have a higher relative activity than the free enzyme at low pH-values and high ionic strengths. Furthermore, the wood samples carrying the enzymes could easily and completely be removed from the reaction solution such that the catalyst could be used for 25 consecutive reaction cycles. The activity is first increasing to its maximum in the eighth cycle. Thereafter, it slightly decreases to a remaining activity of 90% in the 25th cycle. A remaining activity of 90% after 25 cycles is

a remarkable result. Such an extensive reusability could make the system interesting for industrial applications.

Moreover, the anisotropic porous structure of wood allows for a directed liquid flow through the samples. Hence, the enzyme immobilized on wood could be used as a flow-through reactor for continuous-flow biocatalysis. We showed that the yield of the catalyzed reaction is depending on the flow-rate. Lower flow-rates result in an increased yield due to a longer contact time between substrate and catalyst. At higher flow-through rates, however, the higher amount of permeate compensated the lower yield, leading to a similar production rate for all flow-rates tested.

Furthermore, the immobilization method proved to be versatile as it could successfully be applied to other enzymes. We immobilized the enzymes glucose oxidase and peroxidase from horseradish by the same process. With these systems, it was possible to realize a two-step reaction cascade in continuous flow. This could be beneficial for applications in the chemical industry where compounds are synthesized by multi-step reaction pathways.

In general, the easy handling of the system, its multifold reusability and versatility, as well as the possibility to realize continuous flow biocatalysis make the system an interesting alternative to existing systems for multiple applications. The material wood with its natural characteristics, such as anisotropic porosity and mechanical stability, offers a promising green alternative to conventional immobilization scaffolds.

An optimization of the immobilization process, though, might be required for industrial application of the system. By tailoring the immobilization process specifically for the used enzyme, the resulting catalytic activity may be increased. Moreover, chemical modifications of the enzymes prior to the immobilization process might increase the catalyst's performance. For an application in continuous flow, one has to find an appropriate flow-rate that offers the optimal compromise between long contact times and hence high yield on the one side and high throughput on the other side. In addition, further characteristics of the system have to be evaluated if a commercialization is considered. Important characteristics are for example long-term stability of the material, the shelf-life of the membrane reactor as well as the long-term catalytic activity.

The system offers multiple levers for optimization. Firstly, the wood species can be varied to get the desirable pore size distribution. Secondly, other, potentially cheaper, metals could be applied as linker material instead of gold. Lastly, the immobilization procedure can be fine-tuned for the specific enzyme that is used to increase the catalytic activity. Hence, our system opens a toolbox for greener and more sustainable heterogeneous biocatalysts for continuous-flow processes.

Materials and methods

All chemicals were purchased from Sigma-Aldrich and used as received. Glassware was cleaned with *aqua regia* and washed with deionized water to a neutral pH prior to use. The enzymes used were laccase from *Trametes versicolor*, peroxidase from horseradish, and glucose oxidase from *Aspergillus niger*.

Poplar wood sheets were cut with a circular saw to a thickness of 3 mm. From these sheets circular samples with a diameter of 16 mm were produced by punching and subsequently stored in a controlled climate (20 °C, 65% relative humidity) until they were used. The average sample mass was 301.69 ± 9.55 mg, resulting in a density of approximately 0.50 g cm^{-3}.

Production of wood–gold hybrids

Wood samples were stored under vacuum (15 mbar) for 24 hours and subsequently incubated with an aqueous solution of chloroauric acid (HAuCl$_4$, 1.24 mM) at atmospheric pressure for four hours. After the reaction, the wood–gold hybrids were rinsed with water and subsequently dried in an oven at 65 °C overnight.

Production of wood–enzyme composites

Unmodified wood samples or wood–gold hybrids were stored under vacuum (15 mbar) for 24 hours and then incubated with 5 mL per sample of an aqueous solution of enzyme (0.1 mg mL^{-1} enzyme in buffer) at atmospheric pressure for four hours. The wood–enzyme composites were subsequently rinsed with deionized water and then washed three times with a buffer solution for 90 min first, then overnight for 18 h, and finally for 90 min. They were then stored in the buffer solution until they were used. In case of laccase an acetate buffer (pH = 3) was used, whereas a phosphate buffer (pH = 7) was used for HRP and Gox. Buffer concentration was 0.01 M in all cases.

Fluorescence spectroscopy

For the fluorescence labeling 10 mg of the enzyme were dissolved in 5 mL of a buffer solution (NaHCO$_3$/Na$_2$CO$_3$, 1 M, pH = 9). To this solution, 250 µL of a solution of TRITC in DMSO (1 mg mL^{-1}) were added to the enzyme solution and stirred for 3 h. Subsequently, 14 mg of NH$_4$Cl (f.c. 50 mM) were added to quench the labeling reaction. The labeled enzyme was received from the reaction solution by gel-filtration column chromatography after two more hours of stirring.

Fluorescence spectroscopy was executed with a FP-8500 spectrometer from Jasco at an excitation wavelength of 544 nm. The emission spectrum was recorded between 550 nm and 750 nm and the maximal emission was evaluated at a wavelength of 570 nm.

The amount of immobilized enzyme (c_{immob}) was then calculated as the difference between the enzyme concentration before the impregnation (c_0) and after the impregnation (c_1) according to the following equation:

$$c_{immob} = c_0 - c_1$$

Measurement of biocatalytic activity

Biocatalytic activity measurements in a batch procedure were executed by incubating one sample of wood–enzyme composite (f.c. of enzyme 3.57×10^{-8} M) in 5 mL of a solution of ABTS in buffer (0.01 M buffer, 1.00 mM ABTS) for a reaction time of ten minutes. For reaction cycle measurements, the samples were rinsed after each cycle and then immersed into the reaction solution for the next cycle. The concentration of the reaction product ABTS$^+$ was quantified photometrically by measuring its absorbance at a wavelength of 415 nm. Non pH-depending measurements were executed at pH = 3. The buffers used for pH-dependent measurements are listed in Table 3.

For determination of the Michaelis–Menten kinetics, the absorption of the reaction solution was measured in intervals of two minutes for a total reaction time of 20 minutes. These measurements were executed for ten different substrate concentrations. The initial reaction velocities were determined by linear fits of the time-dependent product concentrations. The kinetic parameters could be retrieved by exponential fits of the initial velocities over the substrate concentrations.

All measurements were executed accordingly for free laccase with concentrations of c(laccase) = 2.47×10^{-8} M and c(ABTS) = 0.15 mM.

Continuous-flow biocatalysis

For experiments in continuous flow with immobilized laccase, three samples of wood@Au@lac were mounted in the sample holder (see Fig. S4B†). The flow of the substrate solution (1 mM ABTS in buffer 0.01 M, pH = 3) was then initiated with a Masterflex L/S 7523 peristaltic pump (Cole-Parmer, USA) with a constant flow-rate (4, 6, or 8 mL min^{-1}). The product concentration in the permeate was then determined photometrically in intervals of one minute for ten minutes.

For immobilized HRP and Gox, three samples of wood@Au@Gox were mounted in the sample holder, followed by three samples of wood@Au@HRP. Thereafter, the flow was initiated with a rate of 4 mL min^{-1} and the product concentration of ABTS$^+$ in the permeate was determined for every minute of the first 10 minutes of the reaction. The substrate solution for this experiment consisted of glucose (50 mM) and ABTS (1.8 mM) in buffer (0.01 M, pH = 7).

Further characterization

A Lambda 650 UV/Vis-spectrophotometer of PerkinElmer was used for recording UV/Vis-absorption spectra. The spectra were recorded in a wavelength range of 416 nm to 404 nm in steps of 1 nm with a rate of 4.45 nm s^{-1}. Scanning electron microscopy was carried out on thin-cuts of the wood samples that were sputter coated with platinum/palladium (60/40%) prior to the measurement. Images were acquired with a Quanta 200F from FEI Company at an acceleration voltage of 10 kV. Particle sizes were evaluated by line measurements with the software ImageJ (NIH, USA).

Conflicts of interest

There are no conflicts to declare.

Acknowledgements

References

1 J. N. Armor, *Catal. Today*, 2011, **163**, 3–9.

2 K. Egeblad, J. Rass-Hansen, C. C. Marsden, E. Taarning and C. Hviid Christensen, in *Catalysis*, The Royal Society of Chemistry, 2008, vol. 21, pp. 13–50.

3 A. Schmid, J. S. Dordick, B. Hauer, A. Kiener, M. Wubbolts and B. Witholt, *Nature*, 2001, **409**, 258–268.

4 R. A. Sheldon and J. M. Woodley, *Chem. Rev.*, 2018, **118**, 801–838.

5 B. Gutmann, D. Cantillo and C. O. Kappe, *Angew. Chem., Int. Ed.*, 2015, **54**, 6688–6728.

6 R. Gérardy, R. Morodo, J. Estager, P. Luis, D. P. Debecker and J.-C. M. Monbaliu, *Top. Curr. Chem.*, 2018, **377**, 1.

7 R. A. Sheldon, *Adv. Synth. Catal.*, 2007, **349**, 1289–1307.

8 P. Torres-Salas, A. del Monte-Martinez, B. Cutiño-Avila, B. Rodriguez-Colinas, M. Alcalde, A. O. Ballesteros and F. J. Plou, *Adv. Mater.*, 2011, **23**, 5275–5282.

9 J. Britton, S. Majumdar and G. A. Weiss, *Chem. Soc. Rev.*, 2018, **47**, 5891–5918.

10 A. I. Benítez-Mateos, M. L. Contente, S. Velasco-Lozano, F. Paradisi and F. López-Gallego, *ACS Sustainable Chem. Eng.*, 2018, **6**, 13151–13159.

11 M. L. Contente and F. Paradisi, *ChemBioChem*, 2019, **20**, 2830–2833.

12 M. Planchestainer, M. L. Contente, J. Cassidy, F. Molinari, L. Tamborini and F. Paradisi, *Green Chem.*, 2017, **19**, 372–375.

13 G. Jas and A. Kirschning, *Chem.–Eur. J.*, 2003, **9**, 5708–5723.

14 T. A. Nijhuis, A. E. W. Beers, T. Vergunst, I. Hoek, F. Kapteijn and J. A. Moulijn, *Catal. Rev.*, 2001, **43**, 345–380.

15 A. Cybulski and J. A. Moulijn, *Catal. Rev.*, 1994, **36**, 179–270.

16 J. Wegner, S. Ceylan and A. Kirschning, *Chem. Commun.*, 2011, **47**, 4583–4592.

17 C. P. Haas, T. Müllner, R. Kohns, D. Enke and U. Tallarek, *React. Chem. Eng.*, 2017, **2**, 498–511.

18 N. Brun, A. Babeau Garcia, H. Deleuze, M. F. Achard, C. Sanchez, F. Durand, V. Oestreicher and R. Backov, *Chem. Mater.*, 2010, **22**, 4555–4562.

19 L. Van den Biggelaar, P. Soumillion and D. P. Debecker, *Catalysts*, 2017, **7**, 54.

20 L. van den Biggelaar, P. Soumillion and D. P. Debecker, *RSC Adv.*, 2019, **9**, 18538–18546.

21 H. Wang, Y. Jiang, L. Zhou, Y. He and J. Gao, *J. Mol. Catal. B: Enzym.*, 2013, **96**, 1–5.

22 J. Gao, K. Feng, H. Li, Y. Jiang and L. Zhou, *RSC Adv.*, 2015, **5**, 68601–68609.

23 N. Brun, A. Babeau-Garcia, M.-F. Achard, C. Sanchez, F. Durand, G. Laurent, M. Birot, H. Deleuze and R. Backov, *Energy Environ. Sci.*, 2011, **4**, 2840–2844.

24 B. Sandig and M. R. Buchmeiser, *ChemSusChem*, 2016, **9**, 2917–2921.

25 D. P. Debecker, C. Boissière, G. Laurent, S. Huet, P. Eliaers, C. Sanchez and R. Backov, *Chem. Commun.*, 2015, **51**, 14018–14021.

26 V. Smeets, L. van den Biggelaar, T. Barakat, E. M. Gaigneaux and D. P. Debecker, *ChemCatChem*, 2019, **11**, 1593–1597.

27 F. Svec and J. M. J. Fréchet, *Science*, 1996, **273**, 205–211.

28 E. B. Anderson and M. R. Buchmeiser, *ChemCatChem*, 2012, **4**, 30–44.

29 A. Kirschning, C. Altwicker, G. Dräger, J. Harders, N. Hoffmann, U. Hoffmann, H. Schönfeld, W. Solodenko and U. Kunz, *Angew. Chem., Int. Ed.*, 2001, **40**, 3995–3998.

30 R. Wagenführ, *Holzatlas 6. neu bearbeitete und erweiterte Auflage*, Fachbuchverlag Leipzig im Carl Hanser Verlag, München, 2007.

31 T. Y. Dulneva, L. A. Deremeshko, Y. S. Bilyk, D. D. Kucheruk and V. V. Goncharuk, *J. Water Chem. Technol.*, 2018, **40**, 241–245.

32 M. L. Sens, M. L. Emmendoerfer and L. C. Muller, *Desalin. Water Treat.*, 2015, **53**, 15–26.

33 M. S. H. Boutilier, J. Lee, V. Chambers, V. Venkatesh and R. Karnik, *PLoS One*, 2014, **9**, e89934.

34 S. Vitas, P. Beckmann, B. Skibinski, C. Goldhahn, L. F. Muff and E. Cabane, *Environ. Sci.: Water Res. Technol.*, 2019, **5**, 944–955.

35 S. Vitas, T. Keplinger, N. Reichholf, R. Figi and E. Cabane, *J. Hazard. Mater.*, 2018, **355**, 119–127.

36 Q. Fu, F. Ansari, Q. Zhou and L. A. Berglund, *ACS Nano*, 2018, **12**, 2222–2230.

37 H. Guan, Z. Cheng and X. Wang, *ACS Nano*, 2018, **12**, 10365–10373.

38 M. Vidiella del Blanco, E. J. Fischer and E. Cabane, *Adv. Mater. Interfaces*, 2017, **4**, 1700584.

39 F. Chen, A. S. Gong, M. Zhu, G. Chen, S. D. Lacey, F. Jiang, Y. Li, Y. Wang, J. Dai, Y. Yao, J. Song, B. Liu, K. Fu, S. Das and L. Hu, *ACS Nano*, 2017, **11**, 4275–4282.

40 J. Zdarta, Ł. Klapiszewski, M. Wysokowski, M. Norman, A. Kołodziejczak-Radzimska, D. Moszyński, H. Ehrlich, H. Maciejewski, A. L. Stelling and T. Jesionowski, *Mar. Drugs*, 2015, **13**, 2424–2446.

41 S. Park, S. H. Kim, J. H. Kim, H. Yu, H. J. Kim, Y.-H. Yang, H. Kim, Y. H. Kim, S. H. Ha and S. H. Lee, *J. Mol. Catal. B: Enzym.*, 2015, **119**, 33–39.

42 S. Sulaiman, M. N. Mokhtar, M. N. Naim, A. S. Baharuddin and A. Sulaiman, *Appl. Biochem. Biotechnol.*, 2015, **175**, 1817–1842.

43 V. Incani, C. Danumah and Y. Boluk, *Cellulose*, 2013, **20**, 191–200.

44 C. Goldhahn, I. Burgert and M. Chanana, *Adv. Mater. Interfaces*, 2019, 1900437.

45 M. J. Männel, L. P. Kreuzer, C. Goldhahn, J. Schubert, M. J. Hartl and M. Chanana, *ACS Catal.*, 2017, **7**, 1664–1672.

46 M. H. Zimmermann and A. A. Jeje, *Can. J. Bot.*, 1981, **59**, 1882–1892.

47 D. Fengel and G. Wegener, *Wood : chemistry, ultrastructure, reactions*, Verlag Kessel, Remagen, 2003.

48 M. Fernández-Fernández, M. Á. Sanromán and D. Moldes, *Biotechnol. Adv.*, 2013, **31**, 1808–1825.

49 M.-Y. Ahn, A. R. Zimmerman, C. E. Martínez, D. D. Archibald, J.-M. Bollag and J. Dec, *Enzyme Microb. Technol.*, 2007, **41**, 141–148.

50 H. Qiu, C. Xu, X. Huang, Y. Ding, Y. Qu and P. Gao, *J. Phys. Chem. C*, 2009, **113**, 2521–2525.

51 L. G. Forni, V. O. Mora-Arellano, J. E. Packer and R. L. Willson, *J. Chem. Soc., Faraday Trans. 2*, 1986, 1–6, DOI: 10.1039/P29860000001.

52 I. Dewald, O. Isakin, J. Schubert, T. Kraus and M. Chanana, *J. Phys. Chem. C*, 2015, **119**, 25482–25492.

53 C. Goldhahn, J. Schubert, H. Schlaad, J. K. Ferri, A. Fery and M. Chanana, *Chem. Mater.*, 2018, **30**, 6717–6727.

54 L. P. Kreuzer, M. J. Männel, J. Schubert, R. P. M. Höller and M. Chanana, *ACS Omega*, 2017, **2**, 7305–7312.

55 M. S. Strozyk, M. Chanana, I. Pastoriza-Santos, J. Perez-Juste and L. M. Liz-Marzan, *Adv. Funct. Mater.*, 2012, **22**, 1436–1444.

56 I. Petry, A. Ganesan, A. Pitt, B. D. Moore and P. J. Halling, *Biotechnol. Bioeng.*, 2006, **95**, 984–991.

57 D. Spinelli, E. Fatarella, A. Di Michele and R. Pogni, *Process Biochem.*, 2013, **48**, 218–223.

58 D.-S. Jiang, S.-Y. Long, J. Huang, H.-Y. Xiao and J.-Y. Zhou, *Biochem. Eng. J.*, 2005, **25**, 15–23.

59 A. I. Kallenberg, F. van Rantwijk and R. A. Sheldon, *Adv. Synth. Catal.*, 2005, **347**, 905–926.

60 M.-J. Han, M.-J. Han, H. Choi and H.-G. Song, *Korean Journal of Microbiology*, 2006, **44**, 555–560.

61 R. O. Cristóvão, A. P. M. Tavares, A. I. Brígida, J. M. Loureiro, R. A. R. Boaventura, E. A. Macedo and M. A. Z. Coelho, *J. Mol. Catal. B: Enzym.*, 2011, **72**, 6–12.

62 J. Britton and C. L. Raston, *Chem. Soc. Rev.*, 2017, **46**, 1250–1271.

63 C. Goldhahn, M. Schubert, T. Lüthi, T. Keplinger, I. Burgert and M. Chanana, *ACS Sustainable Chem. Eng.*, 2020, **8**(18), 7205–7213.